Tissue motion tracking at the edges of a radiation treatment field using local optical flow analysis

P T Teo[1, 2] and S Pistorius[1,2,3]
[1]CancerCare Manitoba, 675 McDermot Avenue, Winnipeg, Manitoba, R3E 0V9, Canada.
[2]Department of Physics & Astronomy, University of Manitoba, Winnipeg, Manitoba, R3T 2N2, Canada.
[3]Department of Radiology, University of Manitoba, Winnipeg, Manitoba, R3A 1R9, Canada.

Email: troy.teo@cancercare.mb.ca

Abstract. This paper investigates the feasibility and accuracy of tracking the motion of an intruding organ-at-risk (OAR) at the edges of a treatment field using a local optical flow analysis of electronic portal images. An intruding OAR was simulated by modifying the portal images obtained by irradiating a programmable phantom's lung tumour. A rectangular treatment aperture was assumed and the edges of the beam's eye view (BEV) were partitioned into clusters/grids according to the width of the multi-leaf collimators (MLC). The optical flow velocities were calculated and the motion accuracy in these clusters was analysed. A velocity error of 0.4 ± 1.4 mm/s with a linearity of 1.04 for tracking an object intruding at 10mm/s (max) was obtained.

Keyword: adaptive image-guided radiotherapy, organ intrusion detection, optical flow

1. Introduction

Multi-leaf collimators with leaf positions which are dynamically modified to follow the motion of the target have been proposed [1, 2]. To eliminate errors between the correlation of internal and external surrogates, tracking using electronic portal images (EPI) during beam delivery has been studied [2, 3]. Various marker-less techniques have been proposed for real-time tracking of targets with EPI. Most of these methods require either prior knowledge of the target object or segmentation of the target, such that the delineated contours on the initial image can be used for tracking on subsequent images. To ensure sufficient radiation is delivered to the tumor, the emphasis of these methods is on tracking the tumor. However, studies have shown that discrepancies in the entire dose distribution can arise if the delivery of intensity modulated radiation therapy (IMRT) disregards the motion of the target and normal tissues [4, 5]. For example, during the irradiation of the mammary tissues of breast cancer patients, the ipsilateral lung and heart are often exposed to non-negligible dose. Although the breathing adapted radiotherapy and deep inspiration breath hold technique have been shown to reduce cardiac exposure, some patients were unable to comply with the requirements [6], resulting in unplanned intrusion of OARs into the treatment field. With setup errors and daily variations in organ motion, it is difficult to consistently maintain the OAR outside of the planned radiation field.

Content from this work may be used under the terms of the Creative Commons Attribution 3.0 licence. Any further distribution of this work must maintain attribution to the author(s) and the title of the work, journal citation and DOI.
Published under licence by IOP Publishing Ltd

Detection and tracking of motion close to the leaf edges is challenging. This is partially due to the difficulty in identifying all OARs that could intrude into the treatment beam. As a result, current tracking methods based on apriori information such as template matching might not find an exact match of an intruding OAR. It has been shown that a dynamically-weighted optical flow algorithm can track the global motion of an un-contoured moving target on EPI with an accuracy of 0.4 ± 0.2 mm[7].

This paper aims to investigate the feasibility and accuracy of using a local variant of the optical flow analysis to track motions at the edges of a treatment field without the need to delineate OARs.

2. Methods and Materials

2.1. Image acquisition

A phantom's tumor target placed at a distance of 100 cm from the source was irradiated using a Varian Linac 2100iX 6 MV beam at a dose rate of 600 MU min^{-1}. The target was programmed to move in a periodic pattern with a maximum velocity of 10 mm s^{-1} as described in [7]. A total of 237 EPI, each with an image resolution of 0.391mm/pixel, were collected with a frame rate of 7.5 frames s^{-1}. A duplicate of the image sequence was flipped and concatenated to the original to simulate two objects traveling in the opposite direction and with the same velocity. To simulate the intrusion of objects into the treatment field, a region of 235 pixels by 178 pixels was cropped from the concatenated image matrix, leaving a portion of the flipped target out of the cropped image view (Figure 1).

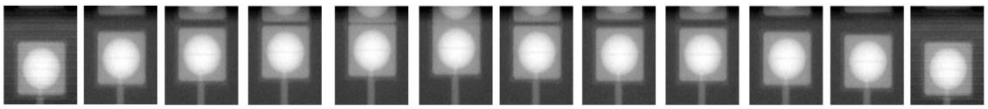


Figure 1. Images with simulated intrusion of object.

2.2. Local optical flow analysis

In this proof-of-concept study, a rectangular treatment aperture is assumed to be bounded by MLC leaf pairs at the top and bottom of the cropped image frame (figure 2). ***Step 1(figure 2):*** The optical flow algorithm was applied to consecutive image pairs to detect and track motions within the treatment aperture. To analyse the local motions near the edges of the treatment aperture, the top and bottom regions were partitioned with horizontal and vertical grids, creating clusters of optical flow vectors. ***Step 2:*** Since each MLC leaf has a width of 3.55 mm at the EPID which is 142.1 cm from source, a nine pixel wide column with a size of 3.52 mm is used for each vertical cluster. With an image size of 178 pixels horizontally, the edge of the image is partitioned into 20 vertical columns. ***Step 3.***For this work each cluster was 9 × 9 pixels in size. Changing the number of pixels within a horizontal cluster would produce a different cluster size that yields different motion estimation. ***Step 4.***The mean and standard deviation of the computed motion were compared as a function of position and velocity. While the tumor is always moving within the treatment aperture, the intruding object, i.e. OAR, only appears in the treatment aperture for a short period of time. The accuracy of tracking the intruding OAR at the edges was obtained by comparing the calculated results with the potentiometer readings when the OAR is present in the image.

3. Results

The estimated velocities for the 20 vertical clusters were observed to be symmetrical about the central column. By way of example, figure 3(a) depicts the velocities of the intruding OAR for the cluster located one row from the top edge of the treatment field and centred horizontally in the 11^{th} vertical column, as shown in Figure 2. Figure 3(b) plots the differences (errors) between the optical flow estimation and potentiometer measurement. The errors between the potentiometer and the computed velocity vary around a mean of zero. A mean error of 0.3± 1.3mm s^{-1} was obtained for the entire image sequence. Figure 3(c) depicts the velocities of the intruding OAR determined for the cluster that is located on the 11^{th} vertical column and two rows away from the edge of the treatment field. A mean error of 0.4± 1.3mm s^{-1} was obtained (figure 3(d)). Figure 4 plots the linear regression between the

measured and computed velocities. A regression coefficient of 0.8 and 1.0 were obtained for the clusters located in row 1 and row 2 respectively.

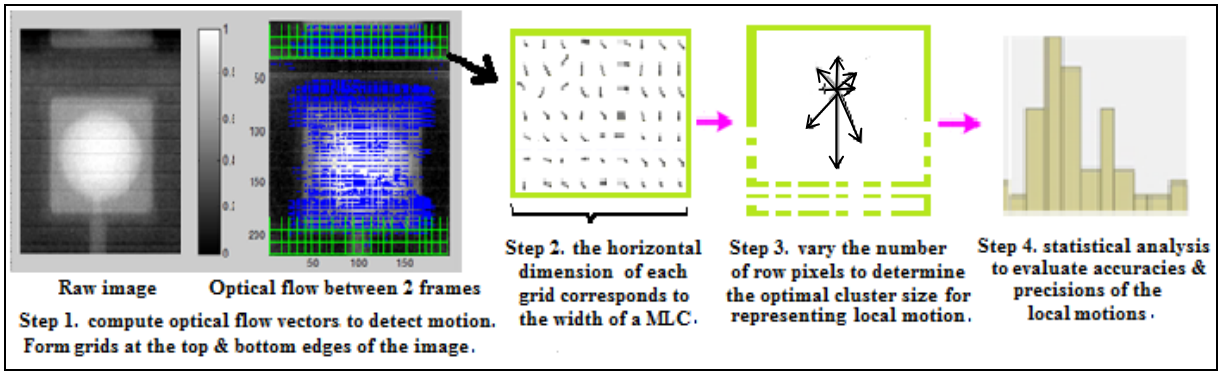


Figure 2. Key steps in determining the variation and statistical significance of the local optical flow vectors at the edges of a radiation treatment field. For this work, each cluster was 9 × 9 pixels in size. Analysis was performed for each of the clusters as a function of position and velocity.

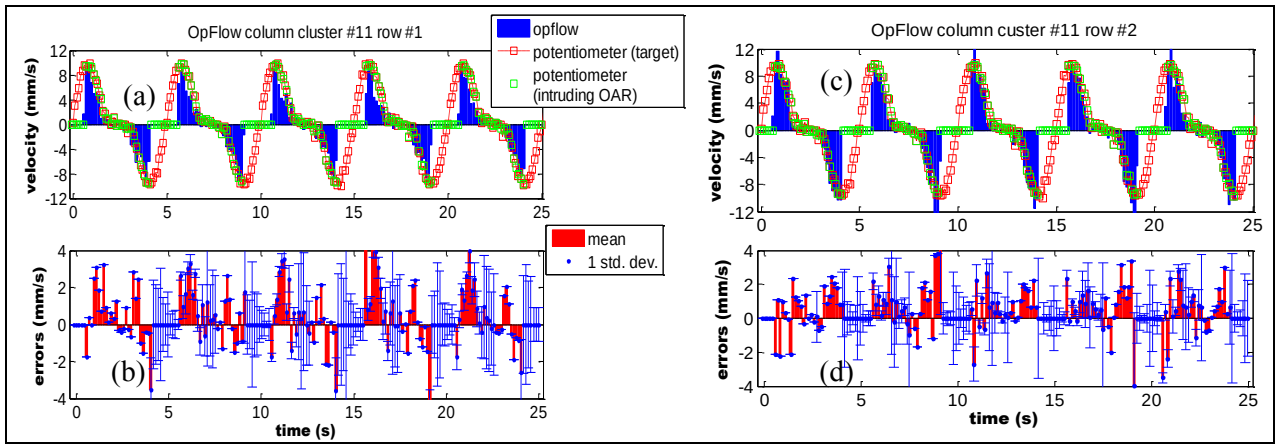


Figure 3.Velocity profiles of the intruding OAR for the cluster located one row (a)-(b) and two rows (c)-(d) from the top edge of the treatment field and centred horizontally in the 11th vertical column. (a) and (c) plots the velocity trajectories; (b) and (d) plots the differences (errors) between the optical flow (opflow) estimation and potentiometer measurement.

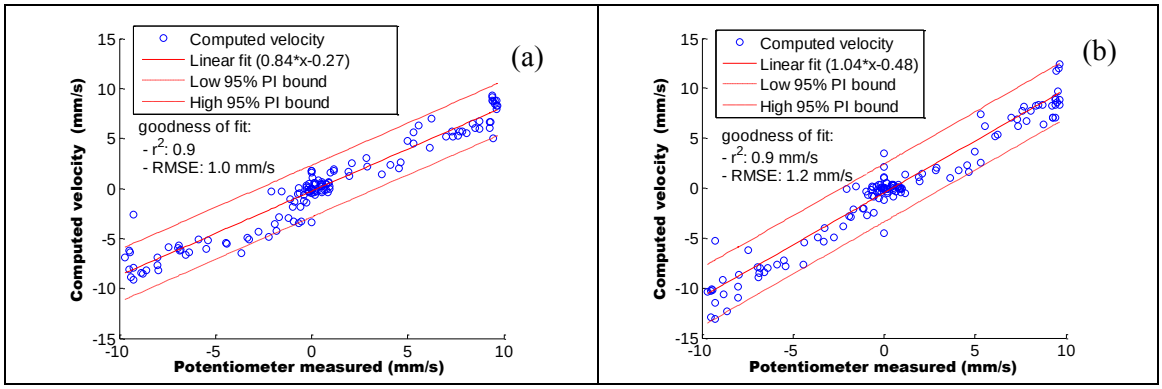


Figure 4. Linear regression analysis to determine the correlation of measured velocities with that detected by the optical flow algorithm for the11th vertical cluster of the 1st row (a) and 2nd row away from the top edges of the treatment aperture respectively.

4. Discussions

Figure 3(b) and 3(d) illustrate that the optical flow tends to overestimate the velocity of the intruding OAR. The linearity between the computed and measured velocity improves for clusters that are further away from the edges (Figure 5). The detection of motion in the first row of clusters can be used to trigger the motion of the MLC leaves to adapt to an incoming OAR. Analysis of the 2nd cluster of pixels can further increase the accuracy with which the direction and magnitude of intrusion is determined.

Further work is required to define the optimal cluster size that would provide an efficient tradeoff between the aperture problem (high motion uncertainties associated with small detection window), noise and the systematic errors due to averaging of larger areas. The combination of local and global tracking [7] to account for main target motions and unplanned intrusions at the edges of a treatment field will be further studied.

For clinical implementation, several challenges can be identified. Firstly, the contrast of the patient anatomy will degrade with respect to the contrast of our phantom. However, the increase in errors, between using a weighted average optical flow to track high contrast objects and objects with a CNR = 5 (which is typical for a clinical portal image) at a velocity of 12 mm/s, is 0.25 mm/s [7]. This is within the uncertainties of this work, and thus the increase in errors for lower contrast clinical images is expected to be minimal. However the patient anatomy will be relatively inhomogeneous in comparison to our phantom object and this structural noise may improve the tracking accuracy. In clinical systems, latencies may be encountered. To realize an adaptive system based on real-time tracking at the treatment edges, prediction algorithms such as the neural network currently being studied by our group, must be implemented.

5. Conclusions

Local optical flow analysis yields a velocity error of 0.4 ± 1.4 mm s^{-1} with a linearity of close to 1 for tracking an object intruding at about 10mm s^{-1} (max). This compares to 0.0 ± 0.5 mm s^{-1} (yielding a mean positional error of 0.4 ± 0.2 mm) for global average tracking. The tradeoff between precision and accuracy can still be improved by optimizing the cluster size. This work demonstrates the feasibility of automatic detection and tracking of intrusion without any pre-defined OAR template or learning data.

References

[1] Keall P J, Kini V R, Vedam S S and Mohan R 2001 Motion adaptive x-ray therapy: a feasibility study *Phys. Med. Biol.* **46** 1–10

[2] Keall P J, Cattell H, Pokhrel D, Dieterich S, Wong K H, Murphy M J, Vedam S S, Wijesooriya K and Mohan R 2006 Geometric accuracy of a real-time target tracking system with dynamic multileaf collimator tracking system *Int. J. Radiat. Oncol. Biol. Phys.* **65** 1579–84

[3] Lin T, Cervino L I, Tang X, Vasconcelos N and Jiang S B 2009 Fluoroscopic tumor tracking for image-guided lung cancer radiotherapy *Phys. Med. Biol.* **54** 981-92

[4] Webb S 2006 Motion effects in (intensity modulated) radiation therapy: a review, *Phys. Med. Biol*. **51** R403-25

[5] McMahon R, Papiez L and Sandison G 2007 Relative motion of tumors and normal tissue during dynamic MIC tracking delivery *Australas. Phys Eng. Sci. Med*. **30 (4)** 331-6

[6] Nissen H D and Appelt A L 2013 Improved heart, lung and target dose with deep inspiration breath hold in a large clinical series of breast cancer patients *Radiother Oncol.* **106(1)** 28-32

[7] Teo P T, Crow R, Van Nest S, Sasaki D and Pistorius S 2013 Tracking lung tumour motion using a dynamically weighted optical flow algorithm and electronic portal imaging device *Meas. Sci. Technol* **24** 074012 (15pp)